Article

Hydrogen, Methane, Brine Flow Behavior, and Saturation in Sandstone Cores During H$_2$ and CH$_4$ Injection and Displacement

Lirong Zhong *, Seunghwan Baek, Mond Guo, Christopher Bagwell and Nicolas Huerta

Pacific Northwest National Laboratory, Energy and Environment Directorate, Richland, WA 99354, USA; seunghwan.baek@pnnl.gov (S.B.); mond.guo@pnnl.gov (M.G.); christopher.bagwell@pnnl.gov (C.B.); nicolas.huerta@pnnl.gov (N.H.)
* Correspondence: lirong.zhong@pnnl.gov; Tel.: +1-509-371-7101

Abstract: Large-scale underground hydrogen storage (UHS) is a critical component in the emerging hydrogen economy. Knowledge of multiphase flow behavior involving hydrogen in storage reservoir formations is crucial to characterizing hydrogen transport properties and essential for the deliverability and storage operations of UHS. There are still many gaps in fully understanding hydrogen–methane–brine multiphase phase flow that require further investigation. In this work, H$_2$ and CH$_4$ were injected through brine-saturated sandstone cores using a tri-axial core holder system fitted with flow rate meters and pressure transducers, while the effluent gas concentrations were analyzed using an online micro gas chromatograph. Brine displacement, permeability, and gas breakthrough curves were measured. We studied the flow behavior of hydrogen and methane in sandstone cores through testing brine displacement by gas injection and comparing the hydrogen displacement of methane with the methane displacement of hydrogen. We also tested the differences between horizontal and vertical flow in brine displacement. The results showed that brine displacement was more efficient in a core with higher permeability and porosity, resulting in a higher initial gas saturation. A higher gas injection rate brought about faster gas breakthrough measured by pore volume and sharper concentration curves. Hydrogen did not exhibit abnormal flow in the sandstone when the flow was horizontal and downward vertical. Gas overriding was observed in brine displacements when the flow was horizontal, with hydrogen showing this behavior more profoundly compared to methane. Downward vertical gas injection induced higher efficiency brine displacement compared to horizontal displacement and resulted in a higher initial gas saturation in the sandstone cores. These findings address critical knowledge gaps regarding gas flow patterns and displacement behaviors during hydrogen injection and recovery phases in UHS facilities using methane as the cushion gas. The insights from this research offer valuable guidance for optimizing UHS systems, ensuring operational efficiency, and advancing sustainable energy solutions in alignment with decarbonization goals.

Keywords: underground hydrogen storage; brine displacement; hydrogen and methane displacement; gravity overriding

1. Introduction

The negative climate effects of accumulating greenhouse gasses, such as methane and carbon dioxide, in our atmosphere has spurred large-scale efforts to reduce emissions and limit global warming to 1.5 °C above pre-industrial levels by 2050 [1]. In response, there has been a notable surge in the exploration of renewable energy sources such as geothermal energy, solar energy, and wind power [2]. These alternatives offer a sustainable pathway for energy production, significantly reducing reliance on fossil fuels and their associated carbon emissions [3].

In this transition, hydrogen has emerged as a promising energy carrier, drawing international attention for its clean, carbon-free attributes and high mass energy density [4–8].

Hydrogen's versatility is further enhanced by its production potential from both conventional and renewable energy sources through various processes such as steam methane reforming and electrolysis [9]. While this dual-source capability improves the economic and operational flexibility of hydrogen production, the versatile usage for transportation fuel, industrial feedstock, residential heating fuel, and fuel for electricity generation positions hydrogen as a pivotal player in reducing pollutant emissions and facilitating the decarbonization of the power sector [3,5]. Putting the roles hydrogen can play alongside renewable energy for decarbonization has brought about the emergence of the hydrogen economy [10].

There are challenges to integrating hydrogen produced from renewable energy sources into the energy system, primarily due to a mismatch between supply and demand. This imbalance is exacerbated by the seasonal nature of some renewable sources, such as wind energy, which could lead to fluctuating hydrogen production levels when energy demand requires a constant supply, such as during winter [1,11,12]. Moreover, the inherent characteristics of hydrogen, being a gas at ambient conditions with a large volume-to-mass ratio, further complicate its storage, necessitating innovative solutions to address discrepancies in supply and demand [1].

Comparing the established practices and infrastructure used for underground natural gas storage can offer valuable insights into potential underground hydrogen storage solutions. Underground hydrogen storage shows great potential for storing large amounts of hydrogen, produced from not only electrolysis and renewable energy, at various time scales for the medium and long term. This offers several advantages [11,12], including reduced surface infrastructure, minimized human exposure to risks, the use of natural storage formations (e.g., porous media), and increased storage density due to higher subsurface pressures. In general, two primary configurations for underground storage are considered [1]: engineered subsurface structures, such as salt caverns and solution-mined rocks, and natural porous rock, including depleted oil and gas reservoirs and saline aquifers. Both configurations have unique benefits and limitations, influencing their suitability based on specific use cases and making them focal points for ongoing research [12].

Leveraging decades of industry experience from underground natural gas storage, similar principles can be applied to hydrogen storage. For example, cushion gas, assumed to stay permanently in the storage reservoir to maintain minimum pressure levels, ensures a consistent supply rate [1,13]. Methane, the primary constituent of natural gas, is considered a viable candidate for cushion gas [1]. Thus, understanding the behavior of gas mixtures (e.g., hydrogen and methane) and multiphase fluids (e.g., the gas mixture and formation water) is key to designing underground hydrogen storage systems and optimizing an operational strategy. Factors influencing hydrogen transport behavior in geological materials include formation properties like porosity, permeability, and heterogeneity; fluid properties like viscosity, density, and buoyance; and mixed properties like dispersity and component fractionation. Core-scale flow behavior directly influences the displacement of the fluids at the reservoir scale and provides inputs needed for accurate simulations and prediction. Further, knowledge of fluid displacement in the hydrogen storage reservoir during H_2 injection and recovery is critical in the design and operation of an underground storage facility. However, while studies have explored important parameters and flow behaviors of multiphase flow in porous media relevant to hydrogen—such as wettability [14], capillary pressure [15], interfacial tension [16], the contact angle [17], relative permeability [15], viscous fingering [18], and gravity overriding [19]—there is scarce research on the behavior of gas mixtures pertinent to underground hydrogen storage. Hence, there are gaps in comprehending the flow behavior of hydrogen gas in the presence of other gas components, such as methane (referred to as cushion gas), and formation water, which necessitate further investigation.

In this research, we studied the flow behavior of hydrogen and methane in sandstone rock cores, tested brine displacement by gas injection, and compared the performance of hydrogen displacing methane with methane displacing hydrogen. The influences of the

rock core and gas injection rate were evaluated. The flow and brine displacement behavior in horizontal and downward vertical directions was compared. This was the first time the characteristics of flushing a methane-filled core with hydrogen (and vice versa) were revealed while measuring the effluent breakthrough concentrations for both gasses. The insights gained from these gas displacement experiments bridge existing knowledge gaps regarding gas flow patterns and displacement behaviors during hydrogen injection and withdrawal phases in storage facilities using methane as the cushion gas.

2. Materials and Methods

2.1. Materials

Ultra-high-purity hydrogen (99.9999%) and pure methane (99.99%) were the testing gasses. Nitrogen (99.99%) was used to flush the lines before switching gasses. Ultra-high-purity argon was the carrier gas for the inline micro gas chromatograph (micro-GC).

A low-salinity brine was used to saturate the core before gas injection. The composition of the brine was NaCl: 2390 mg/L; $CaCl_2 \cdot 2H_2O$: 1100 mg/L; $MgCl_2 \cdot 6H_2O$: 520 mg/L; KCl: 100 mg/L; Na_2SO_4: 70 mg/L; NH_4Cl: 30 mg/L; and $NaHCO_3$: 140 mg/L.

Berea sandstone and Bentheimer sandstone cores 2.54 cm (1 inch) in diameter and 30.48 cm (12 inches) long were the porous media applied in the tests. The measured water permeabilities for the Berea and Bentheimer sandstone cores were 41.93 and 945.06 mD, respectively, and the porosities were 18.08% and 23.78%, respectively.

2.2. Experimental Setup and Test Procedures

2.2.1. Experimental Setup

A multiphase flow testing system was built for this study. H_2 and CH_4 were injected through sandstone cores using a tri-axial core holder system fitted with flow rate meters and pressure transducers, while the effluent gas concentrations were analyzed using an inline micro-GC (Figure 1). This experimental system was used to measure core permeabilities, test brine displacement by gas, and measure gas breakthrough curves during the gas displacement of brine and the gas displacement of gas as a function of the flow rate. In this setup, the core holder could be set in horizontal and vertical orientations. The effluent of the core holder was open to the atmosphere during testing. All injections were conducted with a constant flow rate mode; therefore, the injection pressure was varied as defined by the injection rate, ranging from a few psig to 50 psig (344.8 kPa). All tests were conducted at room temperature.
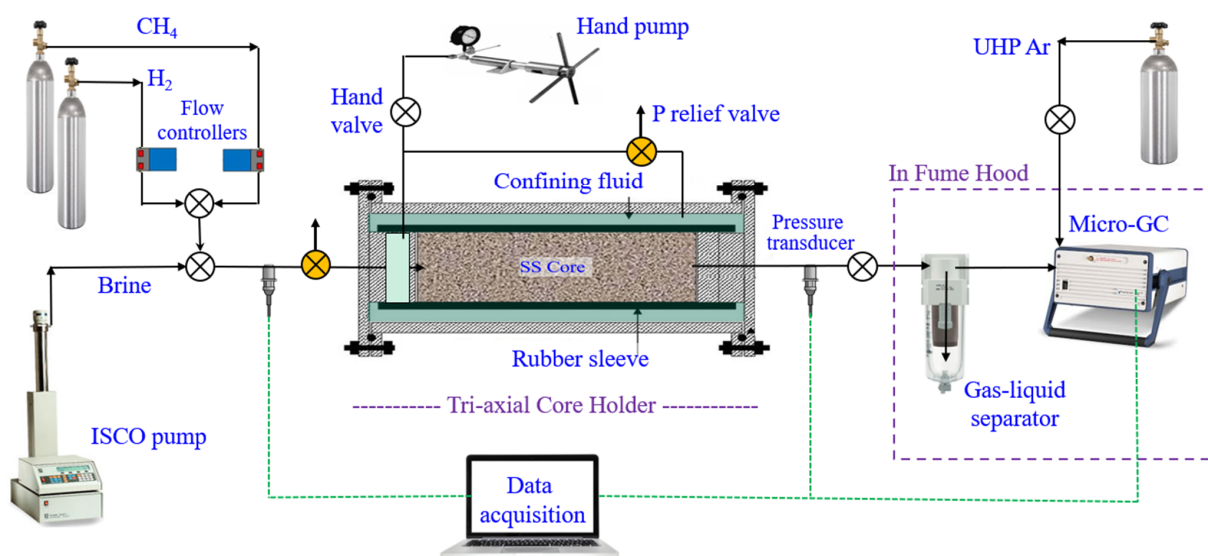
Figure 1. Schematic of the tri-axial core holder testing system with an online micro-GC for measuring H_2 and CH_4. The core holder can be set so that the flow direction is horizontal, as shown in the schematic, or vertical.

2.2.2. Test Procedures

Permeability Tests

First, we pre-saturated the sandstone core to be tested with the low-salinity brine using a vacuum saturation system. The core was then inserted into a Viton sleeve inside the core holder. A confining pressure was applied by pumping water into the confining fluid space with a hand pump. The confining pressure applied was 200 psi (1379.0 kPa) higher than the testing pressure to make sure no flow passed through the gaps between the core and the sleeve. This pressure was kept constant during the test duration. The confining pressure was at least 100 psig higher than the injection pressure to prevent bypassing flow. The brine was injected at different flow rates using an ISCO pump, the pressure was measured at the inflow and effluent ends of the core at each flow rate, and the permeability was calculated.

Brine Displacement Tests

After the core was saturated with brine, hydrogen or methane was injected through the core to displace the brine. Methane or hydrogen injection was started at a desired flow rate controlled by flow controllers to displace brine from the core. Pressures at the inflow and effluent ends of the core holder were recorded and the brine recovery volume in the gas–liquid separator was measured. H_2 and CH_4 concentrations were analyzed using the online micro-GC with the measurement starting at the same time as the gas injection. The micro-GC sampling frequency was 2.25 min per sample.

Gas Displacement Tests

After brine displacement, the pore space in the sandstone core inside the holder was filled with the displacing gas and brine at the residual saturation. The gas in the core was either hydrogen or methane. The other gas was used to displace the current resident gas. The upstream lines were purged with the flushing gas so that a pure gas filled the tubing before the gas displacement was performed. When the flushing gas injection was started, the pressures and the effluent gas concentrations were measured. Gas injection was stopped when the displacing gas concentration in the effluent reached around 100%.

Prior to multiphase flow testing with sandstone cores, baseline testing was performed to verify operational dead volumes and evaluate component influences on the flow and mixing behavior of gasses. In the baseline tests, the core holder was bypassed using stainless steel tubing. This tubing was filled with methane. Hydrogen was then injected into the tubing to displace the methane. Gas compositions were measured with the online micro-GC. Shakedown testing of the experimental system was conducted to quantify the operational range of the gas analyzer and verify data acquisition.

2.3. Test Layout

Besides the baseline tests, eight core flow-through tests were conducted. Table 1 summarizes the tests.

Table 1. List of tests and summary of parameters *.

Test Name	Rock Core	Q (mL/m)	CH.dis. B	H.dis. CH	CH.dis. H	H.dis. B	Flow Hori.	Flow Vert.
Test-01	Berea SS	2.0	x	x			x	
Test-02	Bent. SS	2.0	x	x			x	
Test-03	Berea SS	2.0				x	x	
Test-04	Berea SS	3.0	x	x	x		x	
Test-05	Bent. SS	3.0	x	x	x		x	
Test-06	Berea SS	3.0	x	x	x			x
Test-07	Berea SS	3.0			x	x		x
Test-08	Berea SS	3.0			x	x	x	

* The effluent of the core holder was open to the atmosphere during tests. The injection pressure was varied as defined by the injection rate, ranging from a few psig to 50 psig (344.8 kPa). All tests were conducted at room temperature. SS = sandstone; CH = CH_4; H = H_2; B = brine; dis. = displacing; Bent = Bentheimer; Hori. = horizontal; Vert. = vertical.

3. Results and Discussion

First, baseline testing results are presented to demonstrate the readiness of the experimental system and testing procedures for core flow-through experiments. Second, the initial gas saturation and injection pressure during brine displacement by methane from Berea and Bentheimer sandstone cores in horizontal flow are reported. Third, the breakthrough curves for gas displacing gas from the sandstone cores are compared. Last, the performance of hydrogen displacing brine from sandstone cores in the horizontal and downward vertical flow directions is compared and the resulting H_2 saturation values are reported.

3.1. Gas Recovery Volume in Baseline Testing

It is essential to demonstrate that the testing system is ready for experiments before conducting gas flow-through core tests. When no rock core was inserted into the core holder setup, the volume in the system was fully filled with the initial gas, H_2 or CH_4, with a known volume. In the baseline tests, when H_2 was injected to displace CH_4 or vice versa, the recovery of the initial gas was calculated based on the gas breakthrough curves used to determine the effluent gas concentrations and flow rates.

Figure 2 shows the breakthrough curves for both the H_2 and CH_4 gasses when H_2 was used to displace CH_4 from the core holder system. The known volume of CH_4 in the system was 23.34 mL and the recovered volume was 22.8 mL, with a −2.34% difference. In another baseline test, CH_4 was used to displace H_2 (data shown in Supporting Results, Figure S1). Gas breakthrough curves were compared between the baseline system (i.e., empty core holder) and the system when a sandstone core was installed in the holder. The gas dispersion caused by the core was clearly visible (Figure S2). The difference between the known H_2 volume and the recovery volume was 4.84%. Overall, a good agreement between the operational volume of the experimental system and the calculated displacement volume of effluent gas measurements demonstrates system readiness.
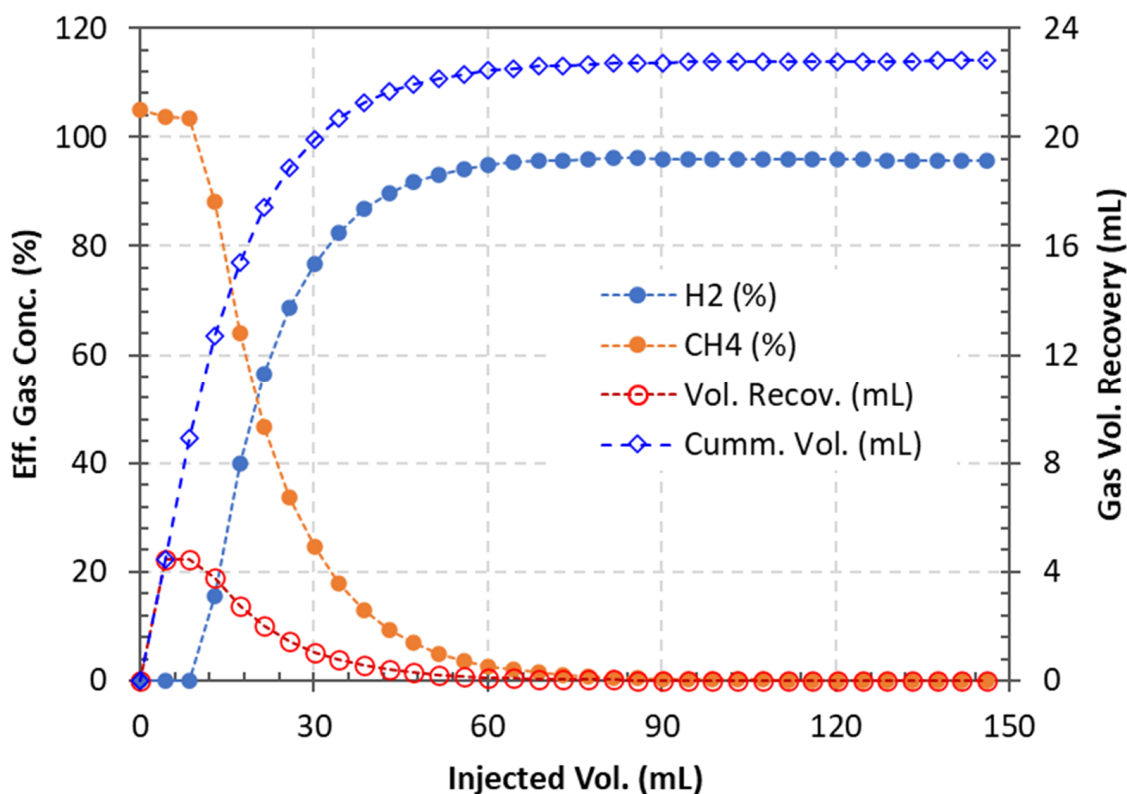

Figure 2. Gas breakthrough curves obtained from H_2 displacing CH_4 in baseline testing. The measured volume of the space filled with CH_4 was 23.34 mL. Based on the effluent CH_4 concentration and flow rate, the calculated CH_4 volume was 22.80 mL.

3.2. Brine Displacement by Methane and the Initial CH₄ Saturation in Sandstone Cores

Figure 3 displays the volume of effluent brine displaced by methane injection and the calculated effluent flow rates for both Berea (left column) and Bentheimer (right column) sandstones and CH_4 injection rates of 2.0 mL/min (top row) and 3.0 mL/min (bottom row). The initial CH_4 saturation in the core was calculated based on the volume of brine displaced from the core by the gas.
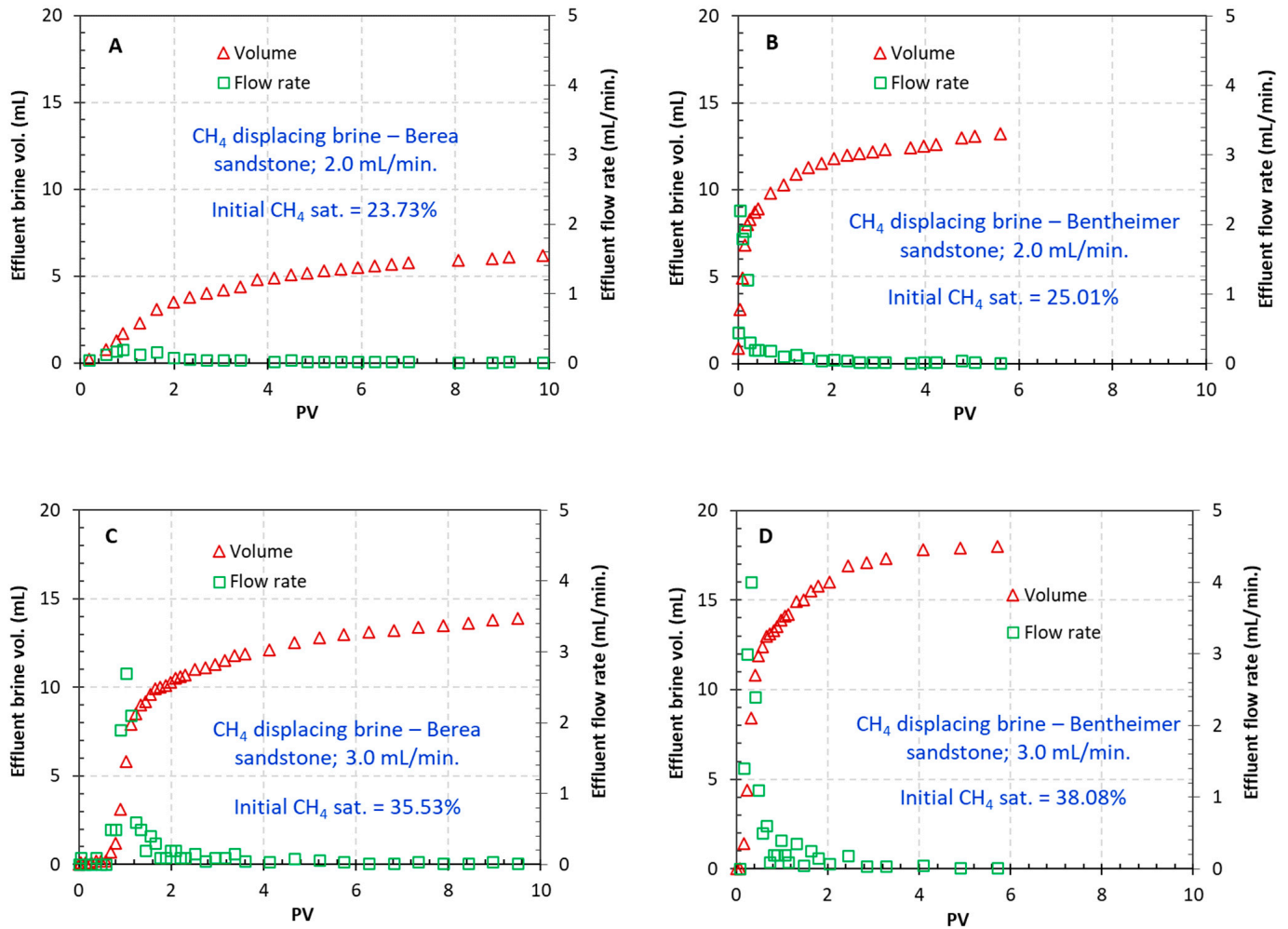

Figure 3. Displaced brine volume, flow rate, and initial CH_4 saturation in sandstone cores. The influence of the gas injection rate and core is compared. PV = pore volume. (**A**) Test-01, (**B**) Test-02, (**C**) Test-04, (**D**) Test-05.

A higher gas injection rate resulted in a larger volume of displaced brine and thus a higher initial gas saturation (Figure 3A vs. Figure 3C and Figure 3B vs. Figure 3D). The peak brine-displacing flow rate was higher at a higher gas injection rate. With the same sandstone core, a higher injection rate induces a higher pore velocity of gas and a greater pressure drop through the core, and thus displaces more fluid filling the pore spaces. Boon and Hajibeygi (2022) [19] reported similar observations when using hydrogen to displace brine from Berea sandstone cores.

At the same gas injection rate, Bentheimer sandstone showed higher initial gas saturations and a higher peak brine displacement rate compared to Berea sandstone (Figure 3A vs. Figure 3B, Figure 3C vs. Figure 3D). The higher gas saturation was attributed to the higher porosity of Bentheimer sandstone. Liu et al. (2017) [20] and Wang et al. (2023) [21] reported similar observations from a set of multiphase core-flooding tests that applied micro-computed tomography scanning systems to monitor fluid saturations in the cores. When the gas injection rates were increased in the same sandstone core, the brine displace-

ment rates and the initial gas saturation were increased (Figure 3A vs. Figure 3C, Figure 3B vs. Figure 3D). The higher flow rates induced higher displacement pressure (Figure 4) and thus improved the brine displacement.
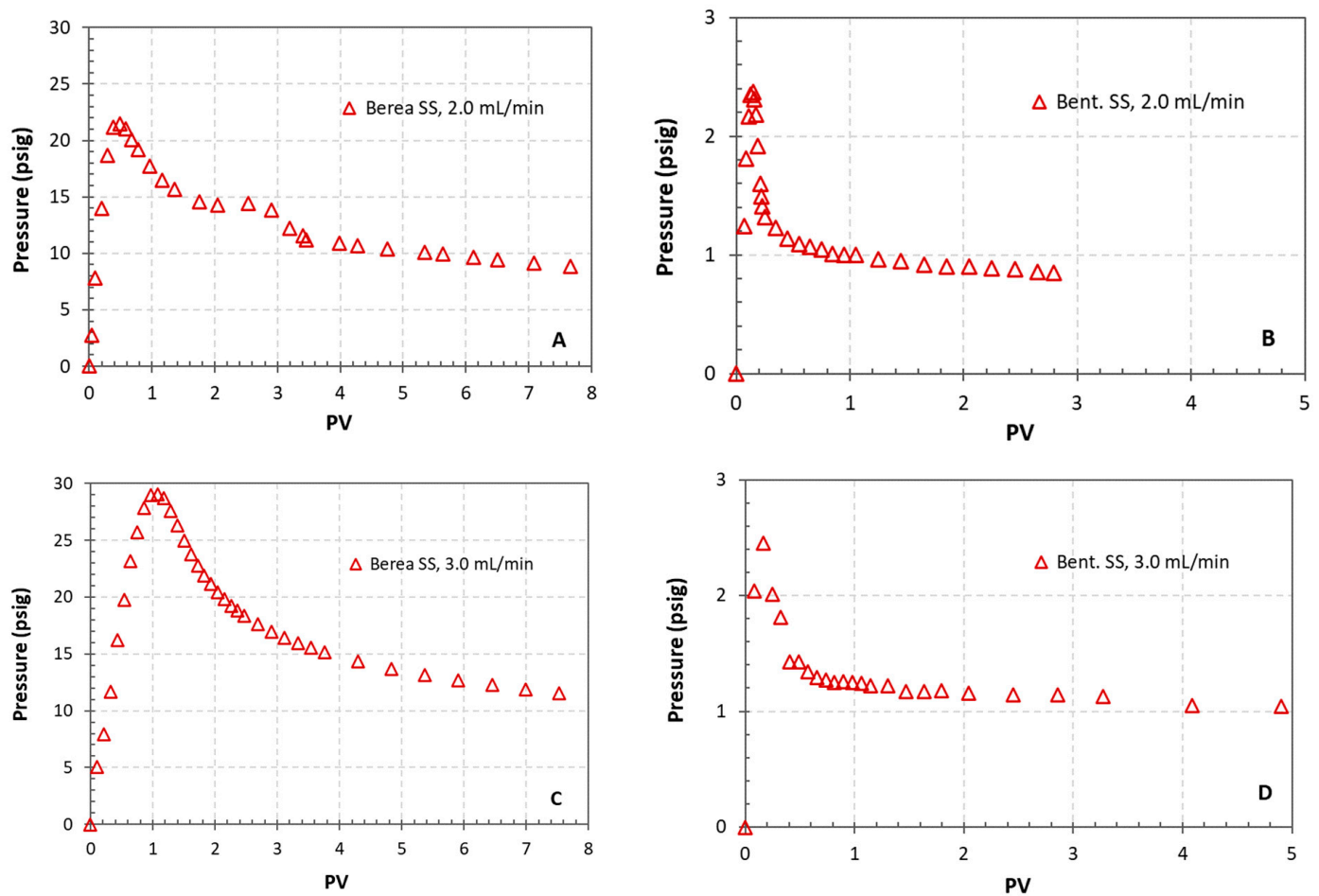
Figure 4. Pressure drops across the sandstone core during gas injection. Methane was injected through Berea sandstone and Bentheimer sandstone cores at a flow rate of 2.0 or 3.0 mL/min. (**A**) CH_4 displacing brine—Berea SS, 2.0 mL/min (Test-01); (**B**) CH_4 displacing brine—Bentheimer SS, 2.0 mL/min (Test-02); (**C**) CH_4 displacing brine—Berea SS, 3.0 mL/min (Test-04); (**D**) CH_4 displacing brine—Bentheimer SS, 3.0 mL/min (Test-05).

3.3. Injection Pressure

Pressure was also measured during brine displacement by methane and the results are shown in Figure 4. The injection pressure is a function of the injection rate, the viscosity of the injectate, and the permeability of the porous medium. When methane was injected into brine-saturated cores, the injection pressure was higher when the injection rate was higher (Figure 4A vs. Figure 4C, Figure 4B vs. Figure 4D). When the gas was injected through the cores at the same flow rate, the Bentheimer sandstone core exhibited lower peak pressure compared to the Berea sandstone. After the gas broke through the core and the pressure drop approached a steady state, Bentheimer sandstone also showed a lower pressure (Figure 4A vs. Figure 4B; Figure 4C vs. Figure 4D) than Berea.

Bentheimer sandstone lost pressure faster than Berea sandstone after the peak pressure, and it took less gas injection for the pressure drop to approach a steady state (Figure 4A vs. Figure 4B; Figure 4C vs. Figure 4D). The characteristic behavior of a faster approaching steady state for Bentheimer sandstone compared to the Berea sandstone was also observed in the brine-displacing process, as exhibited by the accumulative brine volume curves (Figure 3A vs. Figure 3B; Figure 3C vs. Figure 3D).

The differences in permeability and porosity between these two sandstones are behind the observed diversities in pressure behavior. Bentheimer sandstone is more than 10 times more permeable than Berea sandstone, and the porosities are 18.08% and 23.78% for Berea sandstone and Bentheimer sandstone, respectively. Based on Darcy's law for the gas phase [22], a lower gas injection pressure can be obtained when a gas is injected through a higher permeability rock at a fixed flow rate. The higher porosity of Bentheimer sandstone lets the gas flow through the core more easily. Gheshmi et al. (2018) [23] reported that an increase in porosity reduced injection pressure when nitrogen was injected through oil reservoirs. Higher porosity also allows for the quick displacement of brine from the cores (Figure 3) and thus a more rapid decrease in the injection pressure after reaching the peak pressure (Figure 4).

3.4. Hydrogen Displacing Methane—Influence of Flow Rate and Sandstone Core

Figure 5 shows breakthrough curves for gas displacement experiments for both Berea (left column) and Bentheimer (right column) sandstones at different injection rates, 2.0 mL/min (top row) and 3.0 mL/min (middle and bottom rows). The breakthrough curves for H_2 and CH_4 cross at concentrations of about 49% for the tests where hydrogen was used to displace methane (Figure 5A–D). The gas injection rate and the type of sandstone core had minimal influence on the cross-point concentration.

For the same sandstone core, a higher gas injection rate resulted in a faster gas breakthrough in the injected pore volume (PV), as is clearly indicated by the cross-points in the curves (Figure 5A vs. Figure 5C; Figure 5C vs. Figure 5D). As an example, the cross-point of the test with Berea sandstone at a flow rate of 2.0 mL/min was at 1.01 PV and the cross-point of the same core at 3.0 mL/min was at 0.80 PV.

In the test procedure, a constant flow rate was set during gas injection. The inlet pressure increased over time when more gas was injected into the inlet of the core holder. The methane gas saturating the pore space in the core after displacing brine was pushed out when hydrogen injection was started. When the rock core properties were the same, i.e., when injection was applied to the same core, the hydrogen injection rate controlled the change in injection pressure. A higher injection rate not only shortened the time for the pressure to reach the peak value, but also reduced the injected gas volume needed for the pressure to reach this value. Figure 6 shows that when hydrogen was injected to displace methane at flow rates of 2.0 and 3.0 mL/min, the injection pressure peaked at 0.5 and 0.1 PV, respectively. According to Darcy's law for gas phase [22], higher pressure induces a higher flow rate through the core; thus, the pressure data qualitatively explain the earlier breakthrough of the injected gas.

At the same injection rate, Bentheimer sandstone showed earlier gas breakthrough compared to Berea sandstone (Figure 5A vs. Figure 5B; Figure 5C vs. Figure 5D). Because Bentheimer sandstone is more than 10 times more permeable than Berea sandstone, the pressure required to displace gas from the core is much lower based on Darcy's law. The pressure peaked much earlier as shown in the results from the test using hydrogen to displace methane at a flow rate of 3.0 mL/min (Figure 6).

In the experiments using one gas to displace another, the dispersion of one gas into another is revealed by the shape of the breakthrough curves. In the tests presented here with relatively higher flow rates, the dispersion was dominated by the flow velocity [24]. When the gas flow rate was higher, the time available for dispersion in the core was reduced, as observed in the sharper breakthrough curves at higher flow rates (Figure 5A vs. Figure 5C; Figure 5B vs. Figure 5D).
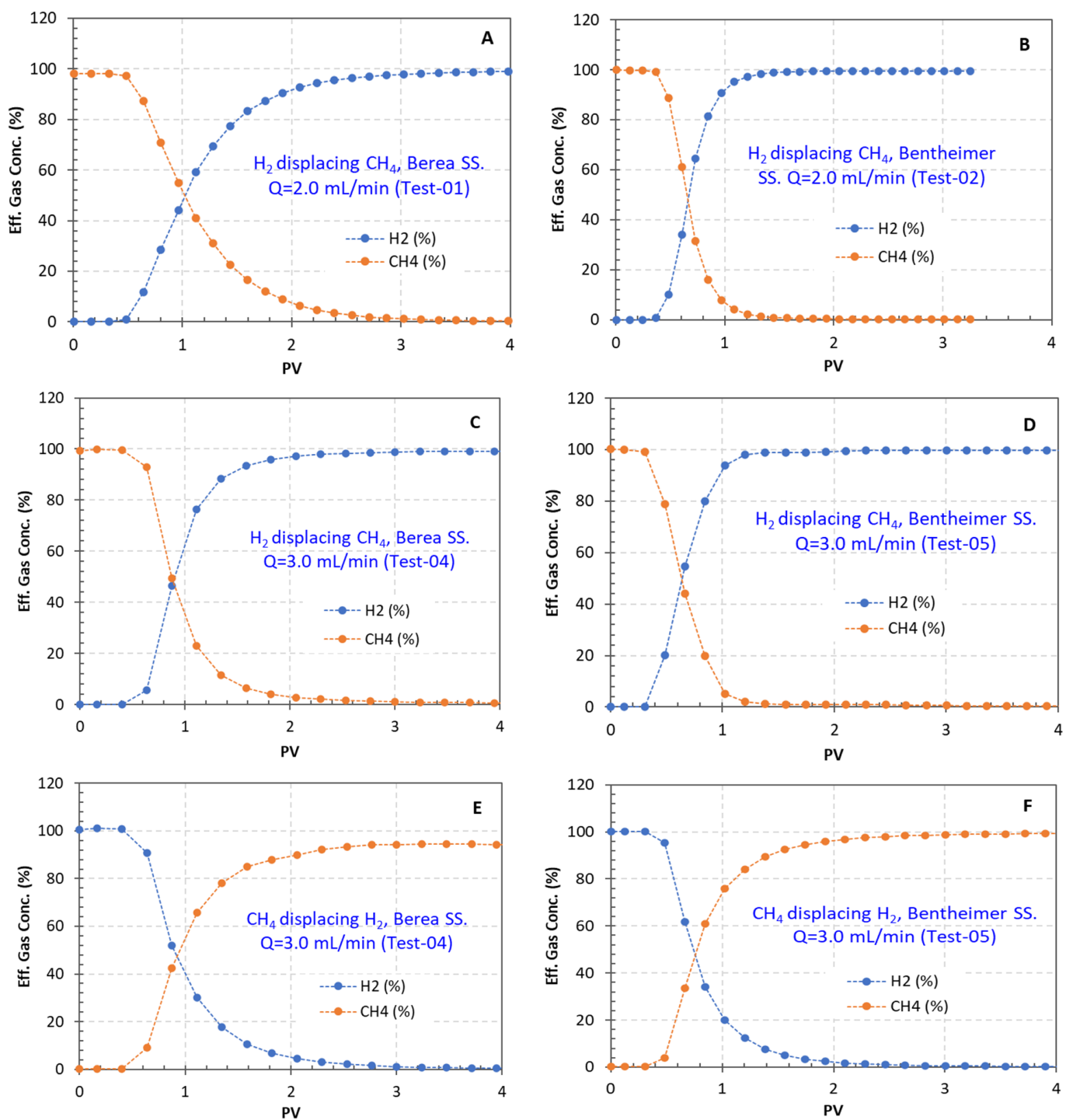
Figure 5. Gas breakthrough curves. (**A**) H$_2$ displacing CH$_4$, Berea SS. Q = 2.0 mL/min (Test-01). (**B**) H$_2$ displacing CH$_4$, Bentheimer SS. Q = 2.0 mL/min (Test-02). (**C**) H$_2$ displacing CH$_4$, Berea SS. Q = 3.0 mL/min (Test-04). (**D**) H$_2$ displacing CH$_4$, Bentheimer SS. Q = 3.0 mL/min (Test-05). (**E**) CH$_4$ displacing H$_2$, Berea SS. Q = 3.0 mL/min (Test-04). (**F**) CH$_4$ displacing H$_2$, Bentheimer SS. Q = 3.0 mL/min (Test-05).
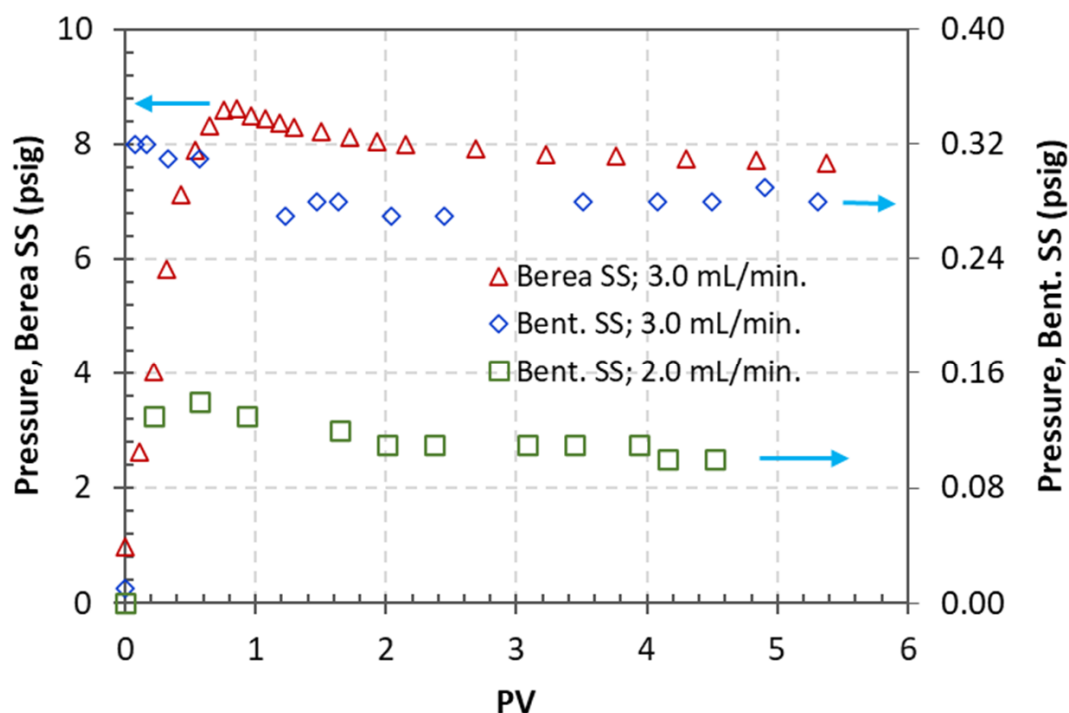
Figure 6. Injection pressures during hydrogen displacement of methane from sandstone cores, illustrating influences of rock cores (Tests 02, 04, 05). The arrows indicate the y-axes for the related data sets.

3.5. Methane Displacing Hydrogen vs. Hydrogen Displacing Methane

Figure 5E,F present the breakthrough curves for tests when methane was applied to displace hydrogen. Comparing Figure 5C with Figure 5E and Figure 5D with Figure 5F, one can see that CH_4 displacing H_2 and H_2 displacing CH_4 exhibited very similar behavior. Breakthrough was earlier for Bentheimer sandstone than Berea sandstone in both processes (i.e., CH_4 displacing H_2 and H_2 displacing CH_4).

The viscosities of H_2 and CH_4 at ambient pressure and room temperature were 0.88×10^{-5} and 1.10×10^{-5} Pa·s, respectively. The densities under the same conditions for H_2 and CH_4 were 0.0899 and 0.717 kg/m^3, respectively. These differences did not cause significant differences in the displacement behavior using either gas to displace the other when the flows were horizontal.

To the best of our knowledge, no studies have been reported in the open literature on using one gas to displace another in porous media while both gas breakthrough curves are recorded. Costanza-Robinson and Brusseau (2002) [25] compared the dispersity of reactive gasses (difluoromethane CH_2F_2 and trichloroethene $CHCl_3$) with a nonreactive gas (methane) in column experiments in which nitrogen was applied as the displacing gas for all the nonreactive and reactive gasses. The effluent concentrations of the displaced gasses were measured but the nitrogen concentration was not recorded. Li et al. (2020) [26] studied gas displacement in sandstone and carbonate cores involving CH_4, CO_2, N_2, N_2O, and He gasses, with a focus on the pore occupancy of these gasses during displacement, but effluent gas concentrations were not measured.

The density, viscosity, and diffusivity of hydrogen are very different compared to other geologically stored gasses such as CO_2, CH_4, and air. Hydrogen's unique properties may result in very special flow behavior in porous media, such as high mobility and increased viscous fingering [27]. Compared to methane and the other nonreactive and reactive gasses tested by Costanza-Robinson and Brusseau (2002) [25], however, hydrogen did not exhibit abnormal flow performance in the sandstone cores as observed in this study when the flow was horizontal.

3.6. Gas Flow Through Brine-Saturated Core: CH₄ vs. H₂

Figure 7 compares the concentrations of the effluent methane and hydrogen gasses during vertical and horizontal brine displacement by these gasses. Berea sandstone was used, and the injection rate was 3.0 mL/min for the experiment. When hydrogen and methane were injected individually to displace brine from sandstone cores in the horizontal flow direction, H_2 breakthrough was earlier compared to CH_4 (Figure 7A). When the displacement was in the downward vertical flow direction, the two gasses had very similar breakthrough times (Figure 7B).
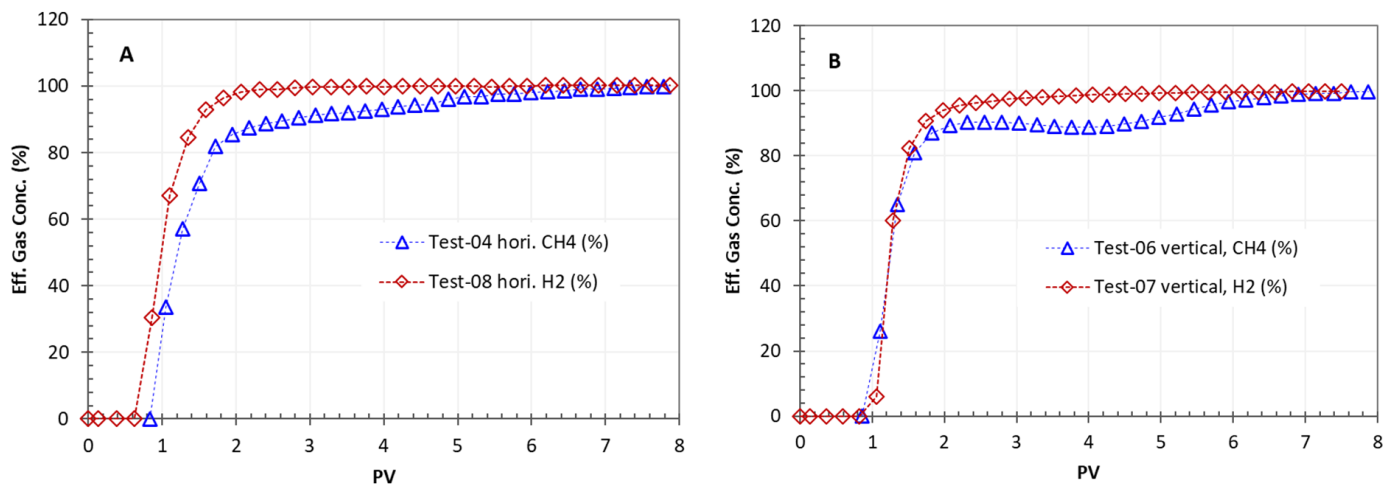
Figure 7. Effluent gas concentrations when hydrogen and methane were used to displace brine from the Berea sandstone core. (**A**) Horizontal flow (Tests 04, 08); (**B**) vertical flow (Tests 06, 07).

When a gas is applied to displace liquid from a porous medium, gravity overriding occurs due to the high-density contrast between the gas and liquid phases, in which the injected gas rises to the top of the formation while the fluid stays at the bottom [19,28,29]. Boon and Hajibeygi (2022) [19] reported gravity segregation when H_2 was applied to displace water from sandstone cores. Gravity overriding causes the by-passing of the fluid being displaced and results in less oil recovery [30] and low sweep efficiency, and thus the low usage of the gas storage formation [31].

The results for the effluent gas concentration showed that H_2 exhibited a higher degree of gravity overriding in horizontal flow compared to CH_4, as evidenced by the earlier breakthrough of the gas (Figure 7). The differences in the viscosity, mass density, and buoyancy force of these two gasses might have caused the observed differences in the flow and brine-displacing behavior. Because H_2 is far less dense than CH_4, the influence of buoyancy will be more pronounced for hydrogen storage than methane storage. The buoyancy driving force that drives gravity override flow for pure hydrogen storage was calculated as 8.4 to 10.3 times greater than that for pure methane storage [31].

The gravity number, $N_g = \Delta\rho g / \nabla P$, defines the ratio between viscous and gravity forces. Here, ∇P (Pa/m) is the pressure gradient, $\Delta\rho$ (kg/m³) is the density difference between fluids, and g (m/s²) is the gravity acceleration. A higher gravity value promotes gravity segregation in the surfactant-alternating gas injection process [30], as shown in Figure 8.
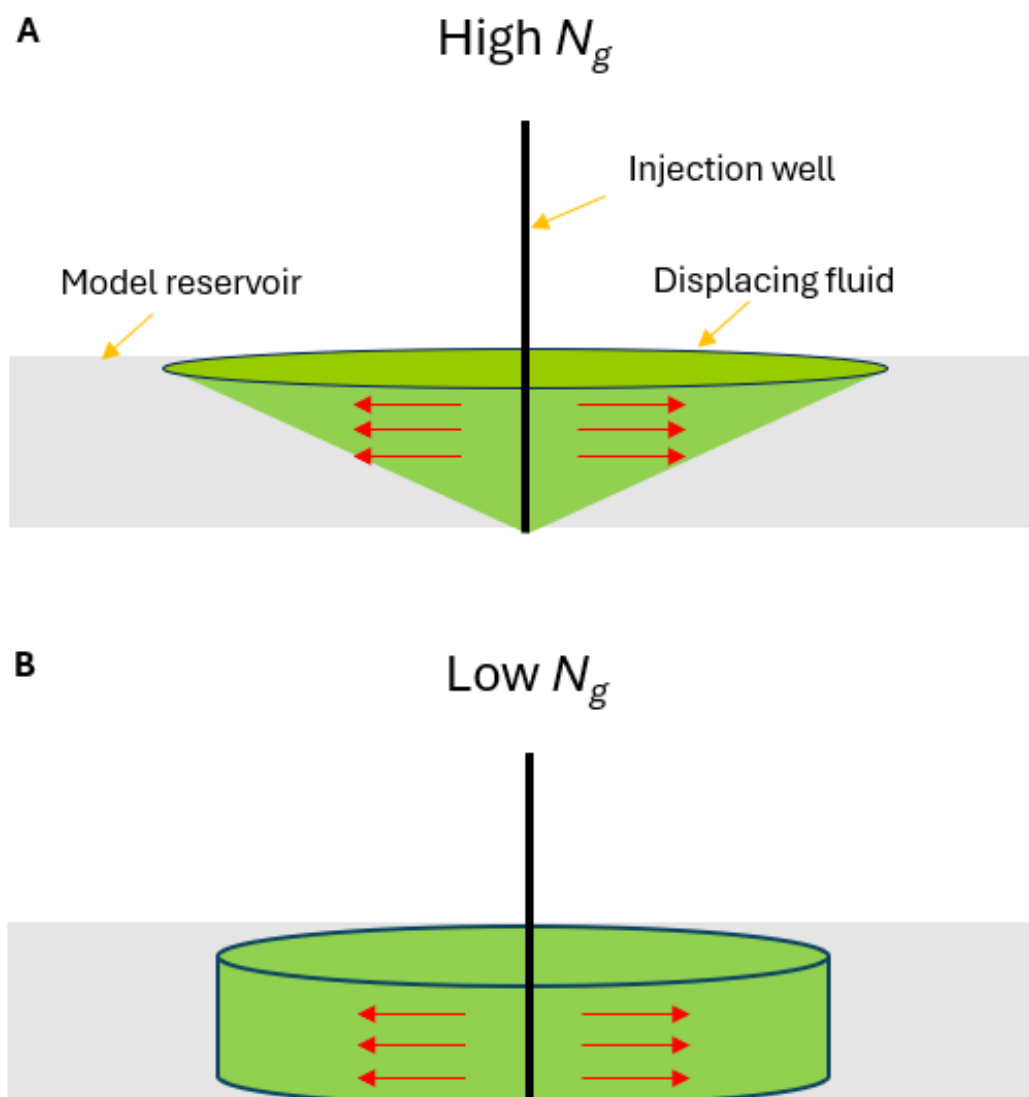
Figure 8. Impact of the gravity number (N_g) on fluid overriding and the reservoir pore utilization. (**A**) Injection with high gravity number; (**B**) injection with low gravity number (modified from [32]).

The calculated *Ng* values were 1.58×10^{-2} and 1.43×10^{-2} for hydrogen and methane injection, respectively. These values are higher than 1.0×10^{-2}, indicating high gravity segregation during brine displacement in porous media [29].

Figure 9 compares the effluent gas concentration in the horizontal flow vs. vertical downward flow directions. Breakthrough for both CH_4 and H_2 occurred slightly earlier in horizontal flow compared to vertical flow. Gas concentrations increased faster after breakthrough in the vertical flow tests as revealed by the slopes of the breakthrough curves.

In horizontal gas injections, the gas overrides brine or other fluids and thus induces a wedge-shaped displacing front as in Figure 8A, resulting in earlier breakthrough. In vertical downward gas injection, a flatter displacing front is formed, inducing sharper breakthrough curves. The differences in displacing behavior are also illustrated in the effluent brine flow and volume accumulations (Figure 10).
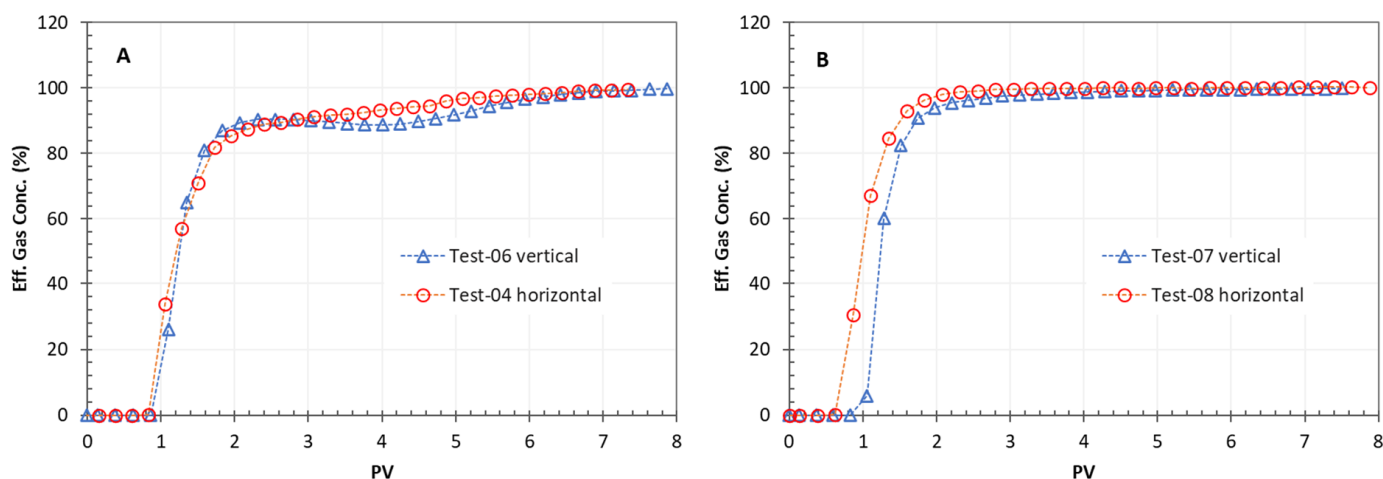
Figure 9. Comparison of effluent gas concentrations during gas displacement of brine: horizontal vs. vertical flow. (**A**) CH_4 displacing brine (Tests 04, 06); (**B**) H_2 displacing brine (Tests 07, 08).
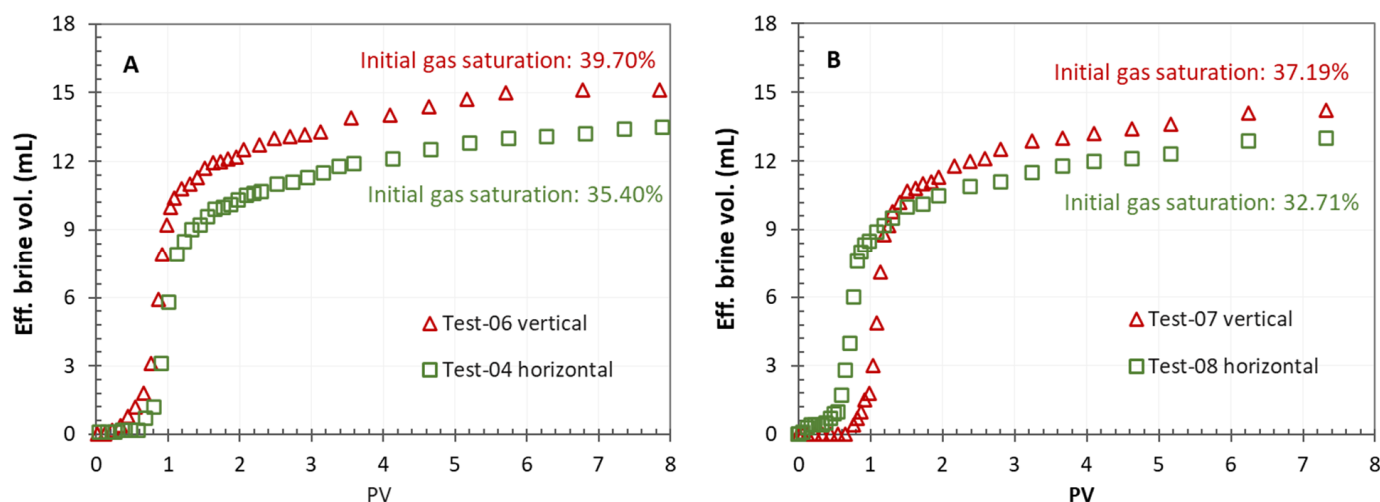
Figure 10. Displaced brine volume comparison during gas displacement of brine from Berea sandstone: horizontal vs. downward vertical flow, all at flow rate of 3.0 mL/min. (**A**) CH_4 displacing brine (Tests 04, 06); (**B**) H_2 displacing brine (Tests 07, 08).

3.7. Vertical and Horizontal Flow Comparison

Downward vertical gas injection through brine-saturated sandstone cores resulted in more efficient brine displacement from the cores compared to horizontal injections for both CH_4 and H_2 gasses (Figure 10). Vertical injection thus produced higher initial gas saturations in the cores. In methane injection, the initial gas saturations were 35.40% and 39.70% for horizontal and vertical injection, respectively. For hydrogen injection, the values were 32.71% and 37.19%, respectively (Figure 10). The brine displacement results clearly indicated that gravity overriding gas flow occurred in the horizontal flow, which induced lower brine displacement from the core. Upward vertical gas injection to displace brine was not tested in this study. Previous work reported lower brine production at the effluent in upward vertical brine displacement compared to horizontal displacement [33].

Fingering is an important factor in hydrogen storage and recovery. Two basic forces, viscosity and gravity, are responsible for fingering in porous media [34]. In horizontal displacement, the gravity force does not affect fingering. When a gas is used to displace brine, gravity is a stabilizing force in downward flow while it is a destabilizing force in upward flow [34]. Thus, upward displacement induces the most profound fingering and

the least efficient brine displacement. In the hydrogen storage process, the downward vertical displacement of brine is strongly recommended.

Initial saturations were higher for methane than hydrogen after brine displacement. The differences might be attributed to the variations in viscosity and density between these two gasses [27].

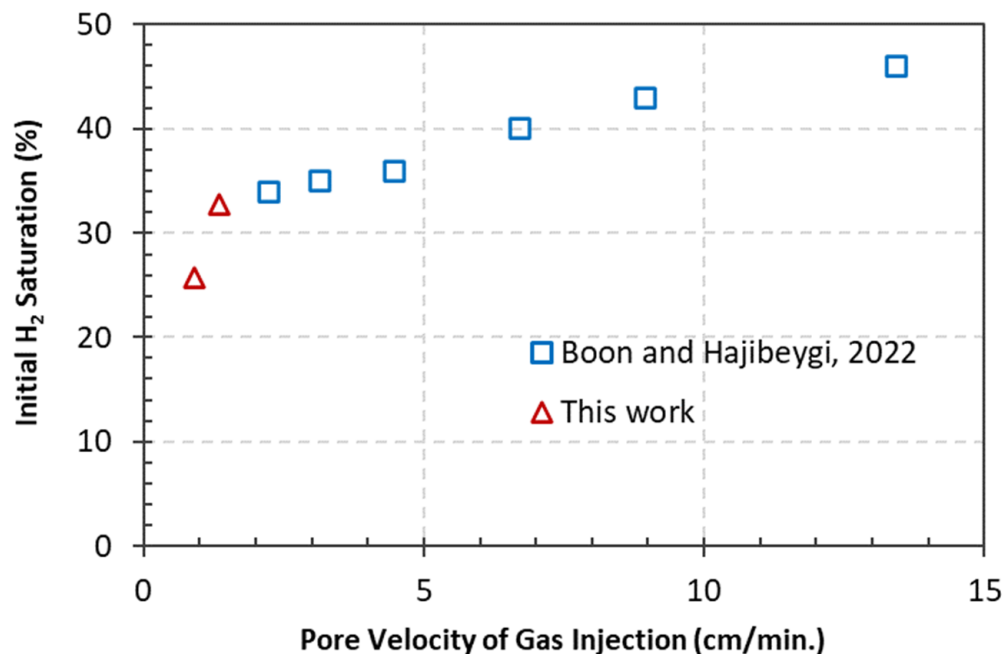### 3.8. Initial Hydrogen Saturation

The initial hydrogen gas saturation, i.e., the percentage of the PV occupied by H_2 after brine displacement by the gas, is an important parameter for underground hydrogen storage since it defines the efficiency of the reservoir usage. A set of values for H_2 saturation in sandstone cores was obtained from recent laboratory studies. Table 2 compares the measured gas saturations obtained in this work with the values reported in the literature.

Table 2. Comparison of the initial hydrogen saturation in sandstone cores between the literature and this study.

Porous Media	Flow Direction; Flow Rate; Injected PV	Saturation Values (%)	References
Berea sandstone (SS) ϕ = 18.08% k = 41.93 × 10^{-15} m^2 Surface area (SA) = 0.93 m^2/g (7.5 PV injection)	Horizontal; 2 mL/min (Test-01) Horizontal; 3 mL/min (Test-04) Vertical (downward); 3 mL/min (Test-07) Eff. at ambient conditions	25.80 32.71 37.19	This study
Fontainebleau SS ϕ = 10.2% k = 200 × 10^{-15} m^2 SA = 0.11 m^2/g (10 PV injection)	Vertical (upward) Under 58 psig pressure	4.5	Al-Yaseri et al., 2022 [35]
Bentheimer SS ϕ = 23–27% k = 1480 × 10^{-15} m^2 SA = 0.45 m^2/g.	Vertical (downward) Under 1450 psig pressure	~36	Jangda et al., 2023 [36] Peksa et al., 2015 [37]
Gosford SS ϕ = 5% k (unknown) SA (unknown)	Orientation and flow direction not reported; 0.01 mL/min 5 PV Ambient conditions	~65	Jha et al., 2021 [17] Roshan et al., 2016 [38]
Berea SS core ϕ = 19.7% k = 203 × 10^{-15} m^2	Horizontal; 5 mL/min; 7 mL/min; 10 mL/min; 15 mL/min; 20 mL/min; 30 mL/min P = 100 bar 3.8 cm core diameter	34 35 36 40 43 46	Boon and Hajibeygi, 2022 [19]
Doddington sandstone k = 170 × 10^{-15} m^2	Vertical (downward); 5 mL/h	20–45	Shahrokhi et al., 2022 [39]

Many factors influence gas saturation, including rock porosity, permeability, the gas injection rate, the gas flow direction in brine displacement, the volume of gas flow through the core, and others. The vertical upward injection of hydrogen displacing brine resulted in the lowest reported H_2 saturation due to the gas flow fingering through the core [35]. Higher gas injection rates resulted in a higher initial gas saturation as shown by Boon and Hajibeygi (2022) [19], consistent with the results of this study (Table 2). The initial methane saturation was also higher at a higher gas injection rate (Figure 3). Vertical downward

displacement resulted in a higher gas saturation than horizontal displacement (Figure 11). Jha et al. (2021) [17] reported an initial hydrogen saturation of ~65%, much higher compared to other studies even though the gas flow rate applied was lower in comparison. The very small core size (5 mm in diameter and 15 mm in length) applied in this core-flooding study might be the cause of the high H_2 saturation [17].

Figure 11. Initial hydrogen saturation in the Berea sandstone core after gas injection at a range of flow rates [19].

Berea sandstone cores were used in Boon and Hajibeygi (2022) [19] and this study, and both studies used horizontal H_2 flow at comparable rates to displace brine (Table 2). Figure 10 compares the initial saturation values for hydrogen obtained in these two studies after converting the gas flow rates into pore velocities. The results of these two studies follow the same trend in the relationship between the flow rate and initial gas saturation.

4. Conclusions

To study the flow behavior of hydrogen and methane gasses in sandstone stone cores and their brine displacement performance, multiphase flow experiments were conducted using a tri-axial core holder setup equipped with an online micro-GC system to analyze the effluent gas concentration. Based on the results of the experiments, we can draw the following conclusions:

- Higher permeability and porosity rock showed quicker breakthrough in brine displacement and a higher initial gas saturation.
- A higher gas injection rate resulted in faster gas breakthrough measured by PV and sharper concentration curves.
- Hydrogen showed similar flow behavior and performance to those of methane in the sandstone cores when the flow was in the horizontal and downward vertical directions.
- Overriding was observed in brine displacements by gasses when the flow was horizontal; hydrogen showed a higher degree of overriding than methane.
- Downward vertical gas injection induced a higher efficiency of brine displacement compared to horizontal displacement, resulting in a higher initial gas saturation in the sandstone cores.

Supplementary Materials: The following supporting information can be downloaded at: https://www.mdpi.com/article/10.3390/en17225800/s1, Figure S1: CH4 displacing H$_2$: tubing + gas separator vol. = 23.34 mL. H$_2$ vol. recovery = 24.47 mL. (off by 4.84%).; Figure S2: Comparison of gas breakthrough concentrations between baseline (BL) and core testing when H$_2$ was used to displace CH$_4$. The dispersion caused by the presence of core is clearly observed.

References

1. Zivar, D.; Kumar, S.; Foroozesh, J. Underground hydrogen storage: A comprehensive review. *Int. J. Hydrogen Energy* **2021**, *46*, 23436–23462. [CrossRef]
2. Pathak, M.; Slade, R.; Pichs-Madruga, R.; Urge-Vorsatz, D.; Shukla, P.R.; Shea, J. Climate Change 2022: Mitigation of Climate Change. In *Working Group III Contribution to the IPCC Sixth Assessment Report: Technical Summary*; Intergovernmental Panel on Climate Change: Geneva, Switzerland, 2022; pp. 51–148.
3. Samsatli, S.; Samsatli, N.J. The role of renewable hydrogen and inter-seasonal storage in decarbonising heat–comprehensive optimisation of future renewable energy value chains. *Appl. Energy* **2019**, *233–234*, 854–893. [CrossRef]
4. Hassanpouryouzband, A.; Joonaki, E.; Edlmann, K.; Haszeldine, R.S. Offshore geological storage of hydrogen: Is this our best option to achieve net-zero? *ACS Energy Lett.* **2021**, *6*, 2181–2186. [CrossRef]
5. Seo, S.-K.; Yun, D.-Y.; Lee, C.-J. Design and optimization of a hydrogen supply chain using a centralized storage model. *Appl. Energy* **2020**, *262*, 114452. [CrossRef]
6. Bauer, S.; Beyer, C.; Dethlefsen, F.; Dietrich, P.; Duttmann, R.; Ebert, M.; Feeser, V.; Görke, U.; Köber, R.; Kolditz, O.; et al. Impacts of the use of the geological subsurface for energy storage: An investigation concept. *Environ. Earth Sci.* **2013**, *70*, 3935–3943. [CrossRef]
7. Sørensen, B. Underground hydrogen storage in geological formations, and comparison with other storage solutions. In *Hydrogen Power Theoretical and Engineering International Symposium*; Merida Technical University: Merida, Mexico, 2007.
8. Uliasz-Misiak, B.; Przybycin, A. Present and future status of underground space use in Poland. *Environ. Earth Sci.* **2016**, *75*, 1430. [CrossRef]
9. Staffell, I.; Scamman, D.; Velazquez Abad, A.; Balcombe, P.; Dodds, P.E.; Ekins, P.; Shah, N.; Ward, K.R. The role of hydrogen and fuel cells in the global energy system. *Energy Environ. Sci.* **2019**, *12*, 463–491. [CrossRef]
10. Bezdek, R.H. The hydrogen economy and jobs of the future. *Renew. Energy Environ. Sustain.* **2019**, *4*. [CrossRef]
11. Baek, S.; Hibbard, L.E.; Huerta, N.J.; Lackey, G.; Goodman, A.; White, J.A. *Enhancing Site Screening for Underground Hydrogen Storage: Qualitative Site Quality Assessment-SHASTA: Subsurface Hydrogen Assessment, Storage, and Technology Acceleration Project*; PNNL-35719; Pacific Northwest National Laboratory: Richland, WA, USA, 2024. [CrossRef]
12. Goodman, A.; Kutchko, B.; Lackey, G.; Gulliver, D.; Strazisar, B.R.; Tinker, K.A.; Wright, R.; Haeri, F.; Huerta, N.; Baek, S. *Subsurface Hydrogen and Natural Gas Storage: State of Knowledge and Research Recommendations Report*; U.S. Department of Energy, Office of Fossil Energy and Carbon Management: Washington, DC, USA, 2022. [CrossRef]
13. Oldenburg, C.M. Carbon dioxide as cushion gas for natural gas storage. *Energy Fuels* **2003**, *17*, 240–246. [CrossRef]
14. Scanziani, A.; Singh, K.; Blunt, M.J.; Guadagnini, A. Automatic method for estimation of in situ effective contact angle from X-ray micro tomography images of two phase flow in porous media. *J. Colloid. Interface Sci.* **2017**, *496*, 51–59. [CrossRef]
15. Yekta, A.; Manceau, J.C.; Gaboreau, S.; Pichavant, M.; Audigane, P. Determination of hydrogen–water relative permeability and capillary pressure in sandstone: Application to underground hydrogen injection in sedimentary formations. *Transp. Porous Media* **2018**, *122*, 333–356. [CrossRef]
16. Chow, Y.T.F.; Maitland, G.C.; Trusler, J.P.M. Interfacial tensions of (H$_2$O + H$_2$) and (H$_2$O + CO$_2$ + H$_2$) systems at temperatures of (298–448) K and pressures up to 45 MPa. *Fluid. Phase Equilibria* **2018**, *475*, 37–44. [CrossRef]
17. Jha, N.K.; Al-Yaseri, A.; Ghasemi, M.; Al-Bayati, D.; Lebedev, M.; Sarmadivaleh, M. Pore scale investigation of hydrogen injection in sandstone via X-ray microtomography. *Int. J. Hydrogen Energy* **2021**, *46*, 34822–34829. [CrossRef]

18. Paterson, L. The implications of fingering in underground hydrogen storage. *Int. J. Hydrogen Energy* **1983**, *8*, 53–59. [CrossRef]

19. Boon, M.; Hajibeygi, H. Experimental characterization of H_2/water multiphase flow in heterogeneous sandstone rock at the core scale relevant for underground hydrogen storage (UHS). *Sci. Rep.* **2022**, *12*, 14604. [CrossRef]

20. Liu, X.J.; Xiong, J.; Liang, L.X.; Yuan, W. Study on the characteristics of pore structure of tight sand based on micro-CT scanning and its influence on fluid flow. *Prog. Geophys.* **2017**, *32*, 1019–1028, (In Chinese with English Abstract).

21. Wang, Z.; Liu, K.; Zhang, C.; Yan, H.; Yu, J.; Yu, B.; Liu, J.; Jiang, T.; Dan, W.; Hu, C. Integral Effects of Porosity, Permeability, and Wettability on Oil–Water Displacement in Low-Permeability Sandstone Reservoirs—Insights from X-ray CT-Monitored Core Flooding Experiments. *Processes* **2023**, *11*, 2786. [CrossRef]

22. Webb, S.W. Gas Transport Mechanisms. In *Gas Transport in Porous Media*; Ho, C., Webb, S., Eds.; Springer: Berlin/Heidelberg, Germany, 2006; Chapter 2; pp. 5–26.

23. Gheshmi, M.S.; Fatahiyan, S.M.; Khanesary, N.T.; Sia, C.W.; Momeni, M.S. Investigating the effects of rock porosity and permeability on the performance of nitrogen injection into a southern Iranian oil reservoirs through neural network. *IOP Conf. Ser. Mater. Sci. Eng.* **2018**, *328*, 012021. [CrossRef]

24. Costanza-Robinson, M.S.; Brusseau, M. Gas-phase Dispersion in Porous Media. In *Gas Transport in Porous Media*; Ho, C., Webb, S., Eds.; Springer: Dordrecht, The Netherlands, 2006; Chapter 7; pp. 121–132.

25. Costanza-Robinson, M.S.; Brusseau, M. Gas phase advection and dispersion in unsaturated porous media. *Water Resour. Res.* **2002**, *38*, 7-1–7-9. [CrossRef]

26. Li, M.; Yang, X.; Connolly, P.; Robinson, N.; May, E.F.; Mahmoud, M.; El-Husseiny, A.; Johns, M.L. Miscible Fluid Displacement in Rock Cores Evaluated with NMR T2 Relaxation Time Measurements. *Ind. Eng. Chem. Res.* **2020**, *59*, 18280–18289. [CrossRef]

27. Heinemann, N.; Alcalde, J.; Miocic, J.M.; Hangx, S.J.; Kallmeyer, J.; Ostertag-Henning, C.; Hassanpouryouzband, A.; Thaysen, E.M.; Strobel, G.J.; Schmidt-Hattenberger, C. Enabling large-scale hydrogen storage in porous media–the scientific challenges. *Energy Environ. Sci.* **2021**, *14*, 853–864. [CrossRef]

28. Stone, H.L. Vertical, Conformance in an Alternating Water-Miscible Gas Flood. SPE-11130-MS. In Proceedings of the SPE Annual Technical Conference and Exhibition, New Orleans, LA, USA, 26–29 September 1982. [CrossRef]

29. Shojaei, M.J.; Osei-Bonsu, K.; Grassia, P.; Shokri, N. Foam flow investigation in 3D-printed porous media: Fingering and gravitational effects. *Ind. Eng. Chem. Res.* **2018**, *57*, 7275–7281. [CrossRef]

30. Shi, J.; Rossen, W. *Improved Surfactant-Alternating-Gas Foam Process to Control Gravity Override*; Society of Petroleum Engineers: Richardson, TX, USA, 1998.

31. Buscheck, T.A.; Goodman, A.; Lackey, G.; Camargo, J.D.T.; Huerta, N.; Haeri, F.; Freeman, G.M.; White, J.A. Underground storage of hydrogen and hydrogen/methane mixtures in porous reservoirs: Influence of reservoir factors and engineering choices on deliverability and storage operations. *Int. J. Hydrogen Energy* **2024**, *49 Pt D*, P1088–P1107. [CrossRef]

32. Baek, S.; Bacon, D.H.; Huerta, N.J. *NRAP-Open-IAM Analytical Reservoir Model-Development and Testing*; PNNL-31418; Pacific Northwest National Laboratory: Richland, WA, USA, 2021. [CrossRef]

33. Adebayo, A.R.; Assad, A.B.; Muhammad, S.K. Effect of Flow Direction on Relative Permeability Curves in Water/Gas Reservoir System: Implications in Geological CO_2 Sequestration. *Geofluids* **2017**, *2017*, 1958463. [CrossRef]

34. Homsy, G.M. Viscous Fingering in Porous Media. *Annu. Rev. Fluid. Mech.* **1987**, *19*, 271–311. [CrossRef]

35. Al-Yaseri, A.; Yekeen, N.; Mahmoud, M.; Kakati, A.; Xie, Q.; Giwelli, A. Thermodynamic characterization of H2-brineshale wettability: Implications for hydrogen storage at subsurface. *Int. J. Hydrogen Energy* **2022**, *47*, 22510–22521. [CrossRef]

36. Jangda, Z.; Menke, H.; Busch, A.; Geiger, S.; Bultreys, T.; Lewis, H.; Singh, K. Singh Pore-scale visualization of hydrogen storage in a sandstone at subsurface pressure and temperature conditions: Trapping, dissolution and wettability. *J. Colloid. Interface Sci.* **2023**, *629*, 316–325. [CrossRef]

37. Peksa, A.E.; Wolf, K.H.A.; Zitha, P.L. Bentheimer sandstone revisited for experimental purposes. *Mar. Pet. Geol.* **2015**, *67*, 701–719. [CrossRef]

38. Roshan, H.; Sari, M.; Arandiyan, H.; Hu, Y.; Mostaghimi, P.; Sarmadivaleh, M.; Masoumi, H.; Veveakis, M.; Iglauer, S.; Regenauer-Lieb, K. Total porosity of tight rocks: A welcome to the heat transfer technique. *Energy Fuels* **2016**, *30*, 10072–10079. [CrossRef]

39. Shahrokhi, O.; Jahanbakhsh, A.; Bakhshi, P.; Andresen, J.M.; Mercedes Maroto-Valer, M. Understanding Multiphase Flow Mechanisms of Hydrogen Storage in Sandstones. In Proceedings of the 16th Greenhouse Gas Control Technologies Conference (GHGT-16), Lyon, France, 23–24 October 2022. [CrossRef]